

Synchrotron radiation hardness studies of
PILATUS IIB. A. Sobott,^{a*} Ch. Broennimann,^c E. F. Eikenberry,^c R. Dinapoli,^b P. Kraft,^b
G. N. Taylor,^a P. R. Willmott,^b C. M. Schlepütz^b and R. P. Rassool^a

Received 11 December 2008

Accepted 20 April 2009

^aSchool of Physics, The University of Melbourne, Melbourne, Victoria 3010, Australia, ^bPaul Scherrer Institute, CH-5232 Villigen, Switzerland, and ^cDECTRIS Ltd, 5400 Baden, Switzerland. E-mail: sbryn@physics.unimelb.edu.au

A synchrotron beam has been used to investigate the radiation tolerance of a PILATUS II module. It has been demonstrated that radiation-induced threshold shifts become significant above 30 Mrad. Individual adjustment of pixel thresholds after irradiation enabled retention of standard behaviour in excess of 40 Mrad. This implies that a module can be continuously irradiated for in excess of 40 days at an individual pixel count rate of 10^6 counts s^{-1} .

© 2009 International Union of Crystallography
Printed in Singapore – all rights reserved**Keywords:** hybrid pixel detector; radiation-induced effects; single-photon counting.

1. Introduction

1.1. Irradiation

Protein crystallography and small-angle X-ray scattering (SAXS) are important applications of synchrotron radiation that require the position and relative intensity of X-ray reflections to be determined to high accuracy. This necessitates the use of detectors with a large detector quantum efficiency, high dynamic range, low noise performance and a small point-spread function. Single-photon-counting pixel detectors such as PILATUS have demonstrated their ability to meet these criteria (Broennimann, Eikenberry *et al.*, 2006).

In contrast to protein crystallography, SAXS measurements frequently require the imaging of elastically scattered features to within a fraction of a degree of the primary beam. This precludes the use of a substantial beamstop, and consequently a high-intensity halo impinges the detector. This configuration can lead to several pixels receiving a high localized dose, particularly if the detector remains stationary throughout consecutive measurements. Thus, it could be surmised that radiation-induced effects may lead to a reduction in detector homogeneity.

Therefore the effect of high dose on a PILATUS II module has been investigated on a pixel-by-pixel basis. Methods for restoration of detector homogeneity by compensation of radiation-induced effects are also presented.

1.2. System description

A PILATUS II module comprises a single 320 μm -thick silicon sensor bump-bonded to an array of readout channels. The monolithic sensor consists of an array of square pn-diodes, of side length 172 μm , with each diode electrically connected *via* a 15–25 μm indium ball to a readout channel. Charge liberated by X-rays interacting with each detecting element is delivered *via* the bump-bond interconnection

(Broennimann, Glaus *et al.*, 2006) to a preamplifier, shaper and leading-edge discriminator. If the incoming charge exceeds a pre-defined threshold, a local counter is incremented. This approach results in a completely digital storage of the number of detected X-rays at the pixel level (Broennimann *et al.*, 2000). Each individual pixel of a module's entire $487 \times 195 = 94965$ pixels is able to individually record single photon events. However, the location of the CMOS readout chip directly behind the sensor places it directly in the path of the incoming X-rays. This can lead to a substantial received dose. For example, at 12 keV approximately 25% of incident X-rays undergo transmission. Consequently, the PILATUS II readout chip, that has been designed using a standard commercial CMOS process, was hardened with special layout techniques.

This paper reports on investigations of the changes induced in PILATUS II by localized doses of up to 150 Mrad and their effect on detector homogeneity. Flat-field illuminations and threshold scans were implemented to investigate variations in the sensor and readout chip, respectively.

2. Effects of irradiation

2.1. Radiation-induced effects on sensor

Radiation-induced effects on the sensor can be categorized into bulk and surface defects. Bulk damage involves the displacement of crystal atoms, which can lead to a change in the sensor's electrical properties. However, this requires a minimum recoil energy of 25 eV (van Lint *et al.*, 1980), which precludes the induction of bulk damage by 12 keV X-rays. Surface damage includes changes in the covering dielectrics and the interface region, the most important of which is an increase in the oxide charge (Rossi *et al.*, 2006). Sensor damage manifests itself as an increase in leakage current and

charge trapping and can also lead to space charge sign inversion and a subsequent rise in full depletion voltage. As detector homogeneity is paramount in SAXS measurements, this study focused on quantizing the radiation-induced change, not the responsible mechanisms.

2.2. Radiation-induced effects on CMOS

Radiation-induced transistor parameter shifts can greatly affect the analog front end of hybrid pixel detectors. Prior studies have revealed that even a moderate radiation dose of approximately 10 krad (Llopart, 2007) can induce a large deviation from nominal chip behaviour. Consequently, PILATUS was designed utilizing radiation-tolerant layout techniques (Anelli, 2000; Dinapoli, 2004). Ionized electrons generated in the vicinity of the transistor's oxide quickly dissipate, but holes, owing to a mobility of five to 12 orders of magnitude less (Anelli, 2000), are often trapped. Total threshold shift is related to both the density of holes trapped in the oxide and the charge state of traps at the silicon–oxide interface (McLean *et al.*, 1989; Winoukur, 1989). The interface states induce a negative shift for a p-channel transistor and a positive shift for an n-channel transistor, thus always increasing the value of the absolute threshold. Conversely, oxide-trapped charge increases the absolute value of the threshold voltage for p-channel MOS transistors while decreasing it for an n-channel MOS. Consequently, radiation-induced effects serve to always increase the threshold voltage absolute value for p-channel MOS transistors, while it can be positive or negative for n-channel transistors. Owing to the configuration of the PILATUS preamplifier, this has the effect of always increasing gain and reducing speed.

In PILATUS II, p- and n-channel transistors are responsible for establishing the operating point of the amplifier stages of the pre-amplifier and shaper, respectively.

2.3. Trimming, flat-field prior to irradiation

The threshold trim adjustment procedure, or threshold trimming, has been previously described in detail (Eikenberry *et al.*, 2003). Briefly, the threshold level is globally controlled by a chip-wide comparator voltage, V_{cmp} , and compensated by a local 6-bit digital-to-analog converter (DAC) on a per pixel basis. The analog output range of the DAC is controlled by a module-wide voltage, V_{trim} .

The trimming process is best performed with the detector immersed in a homogeneous field of monochromatic X-rays. Individual discriminator levels are then scanned using the global threshold and a correction voltage specific to each pixel. The threshold voltage is then adjusted on a pixel-by-pixel basis to half the beam energy to minimize the influence of charge sharing between pixels (Broennimann *et al.*, 2000). However, X-rays undergoing conversion in close proximity to pixel boundaries, particularly corners, may not liberate sufficient charge to be counted by the discriminator and therefore go unregistered. Consequently, quoted dose values represent the lower bound of the actual dose received.

Inhomogeneities in charge collection over the pixel array lead to differences in pixel sensitivity. This is primarily due to subtle variations in the pixels' effective detective volume, *i.e.* the region where incident X-rays undergo conversion. Although not a symptom of threshold value, sensitivity variations can be compensated for by trimming the detector.

Detector illumination with a homogeneous monochromatic X-ray field ('flat-field') allows subtle variations in pixel sensitivity to be investigated. This method, undertaken prior to and post-irradiation, has been exploited to determine whether irradiation changes pixel sensitivity. A detailed description of the flat-field procedure can be found by Schlepütz *et al.* (2005).

3. Experiment

3.1. Beamline

Dose deposition was undertaken at the Materials Science beamline (Patterson *et al.*, 2005), Swiss Light Source, Paul Scherrer Institut, utilizing 12 keV synchrotron radiation. An EPICS (experimental physics and industrial control system) script was implemented to translate unattenuated focused beam across the module in discrete steps, irradiating the detector with approximately 2×10^{12} photons $\text{s}^{-1} \text{mm}^{-2}$. Exposure time was varied in order to control the accumulated incident flux. An exposure time of 256 s resulted in the maximum accumulated incident flux of approximately 1.8×10^{13} photons in an individual pixel.

3.2. Dose distribution

In normal operation, photon-counting detectors allow a direct measurement of per-pixel deposited dose,

$$D = \frac{E_x N_x}{m_p} = 8.73 \times 10^{-6} N_x, \quad (1)$$

where N_x is the number of counts per pixel, E_x is the photon energy and m_p is the pixel mass. However, in these radiation damage studies a deposition rate exceeding 10^{10} photons $\text{pixel}^{-1} \text{s}^{-1}$ leads to paralysis of central pixels. An accumulated incident flux map was therefore achieved by first calibrating a series of attenuators in the detector's linear regime. For each deposition step, the distribution of the beam intensity through the calibrated attenuators was first recorded to serve as a reference image. Removal of the calibrated attenuators then enabled dose deposition, with the corresponding accumulated incident flux map calculated *via* extrapolation of the reference image. Fig. 1 was obtained by summing the accumulated incident flux map for each irradiation step and therefore represents the accumulated incident flux distribution received by the entire module. The corresponding dose was then calculated on a pixel-by-pixel basis *via* the multiplicative constant yielded in equation (1).

As a consequence of this approach, quoted doses refer to the total dose received by the sensor, not the readout chip. X-ray monochromaticity ensures that transmission, and therefore the dose received by the underlying chip, is constant

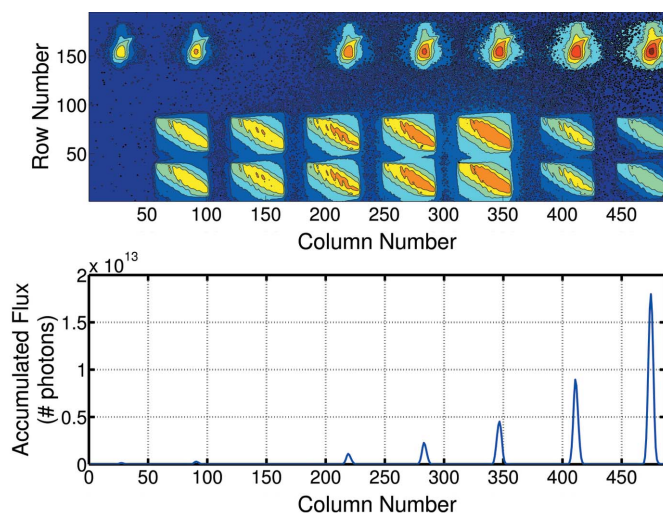


Figure 1 Obtained by summing the individual exposures undertaken at each irradiation step, the upper image depicts the accumulated flux distribution on the module. A cross section taken along row 155 transverses the highest accumulated flux regions and indicates that the maximum number of photons incident on a pixel is approximately 1.8×10^{13} . Analysis was constrained to the four regions above column 250 and row 120, as other regions received insufficient accumulated flux, and therefore dose, to induce a measurable change.

at approximately 25%. Analysis was constrained to the four highest accumulated flux regions, as other regions received insufficient flux, and therefore dose, to induce a measurable change.

4. Analysis

4.1. Flat-field evaluation

A series of flat-field images were recorded prior to and post-irradiation. These were used to investigate changes in pixel sensitivity induced by the irradiation procedure. Results of these measurements are shown in Fig. 2, which was obtained by dividing a post-irradiation flat-field by that of a pre-irradiation flat-field. An increase in count-rate ratio indicates that irradiation causes an increase in pixel sensitivity. However, for a deposited dose of less than 80 Mrad, pixels can be returned to standard behaviour by re-trimming post-irradiation, as evidenced by Fig. 3. As the sensor does not absorb 100% of incident radiation, the doses quoted are accumulated by both the sensor and readout chip.

4.1.1. Comparator calibration. Threshold scans at multiple energies were undertaken to calibrate individual comparators with respect to energy post-irradiation. Heavily irradiated pixels exhibited a substantial gain change from 55.6 mV keV^{-1} , for a typical un-irradiated pixel, to 93.6 mV keV^{-1} , as evident in Fig. 4. Total gain is a function of the gain of the preamplifier and the gain of the shaper, which are realised by basically the same circuit. The slight variation in offset is ascribed to threshold shifts in the comparator, but could also be explained by a small DC shift at the shaper output. Preamplifier gain is a function of V_{rf} , an externally controllable voltage governing feedback in the preamplifier, V_{th} , the

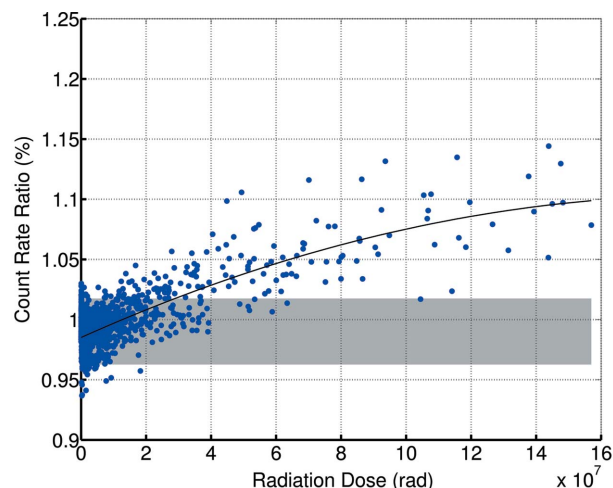


Figure 2 Flat-field response obtained by dividing a post-irradiation flat-field by that of a pre-irradiation flat-field, without trimming. Each data point represents a pixel; however, analysis was constrained to the four highest-dose regions of Fig. 1. A shaded 2σ variation band, representing the count-rate dispersion of un-irradiated pixels, has been used in conjunction with an indicative trend line to approximate the dose required to induce departure from nominal sensor behaviour. Irradiation clearly increases pixel sensitivity.

feedback transistor threshold voltage, and V_0 , the output voltage,

$$g = -f [V_{rf} - |V_{th}| - V_0]. \quad (2)$$

As $[V_{rf} - |V_{th}| - V_0]$ decreases, the circuit slows, thereby reducing ballistic deficit. This results in an increased pulse for the same input charge. Clearly, a radiation-induced increase in the absolute value of the threshold voltage will increase the gain of the preamplifier; however, this effect can be negated by judicious selection of the external voltage V_{rf} .

A key feature afforded by PILATUS is the ability to directly monitor the analog response of the front end to incoming charge. This allows the radiation effects in the

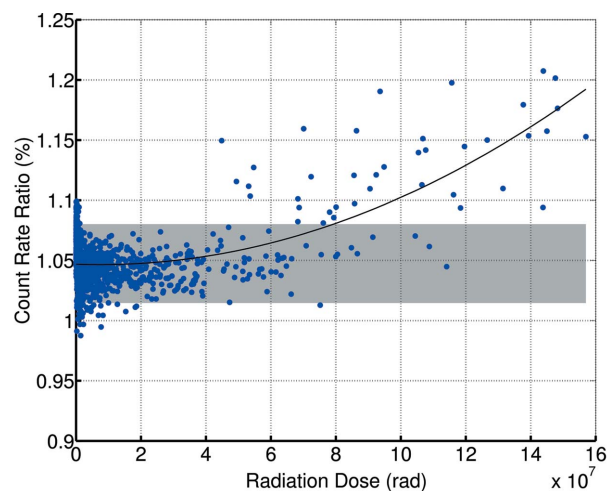


Figure 3 Count-rate variation dependence on dose. The plot was obtained by division of trimmed flat-field response post-irradiation by trimmed flat-field response before irradiation. The indicative trend line departs the 2σ variation band at approximately 80 Mrad.

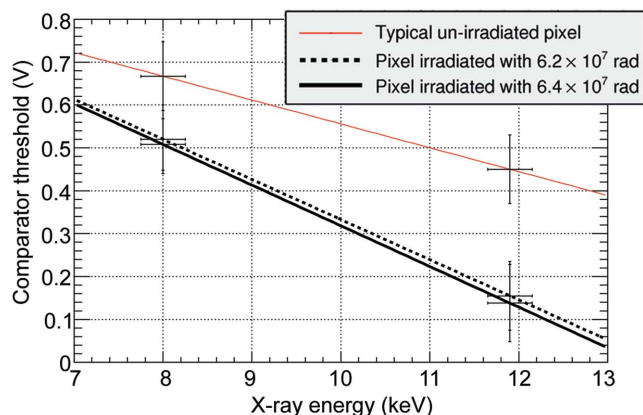


Figure 4 Comparator calibration plots for irradiated and un-irradiated pixels. The substantial increase in gain and offset is assigned to voltage shifts in the analog front end and comparator, respectively.

preamplifier and shaper to be examined independently of those in the discriminator. Incrementation of V_{rf} whilst monitoring analog out indicated that a shift of 50 mV is required to return the gain of the heavily irradiated pixels to that of the un-irradiated pixels. Conversely, decrementing V_{rf} of the un-irradiated pixel by 50 mV resulted in an analog response similar to an irradiated pixel.

Although the main effect on the performance of the PILATUS preamplifier and shaper is caused by a threshold shift in p-type transistors, circuit simulations show, and measurements confirm, that the threshold voltage shift of n-type transistors is also playing a role in the post-irradiation behaviour of the chip.

4.1.2. Dose-dependent threshold shifts. To decouple the effects of radiation damage on the trimming circuitry, threshold scans were undertaken prior and post-irradiation solely using the global threshold. The resulting difference is shown on a pixel-by-pixel basis in Fig. 5. As delta threshold is the threshold before irradiation minus that post-irradiation,

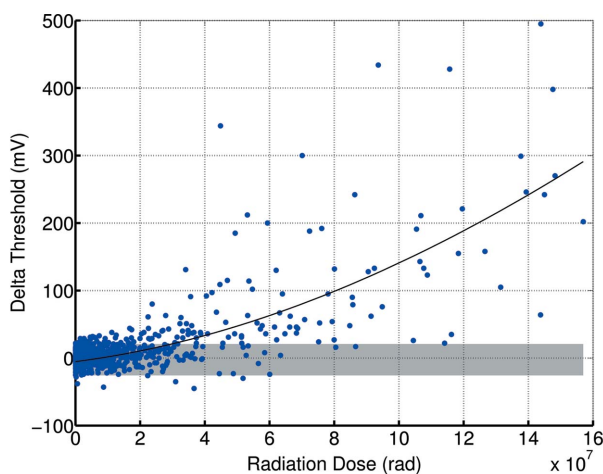


Figure 5 Change in threshold as a function of dose, without trimming. The indicative trend line departs the variation band at approximately 30 Mrad. It is therefore considered that, for the majority of pixels receiving 30 Mrad, the induced threshold shift will cause departure from normal behaviour.

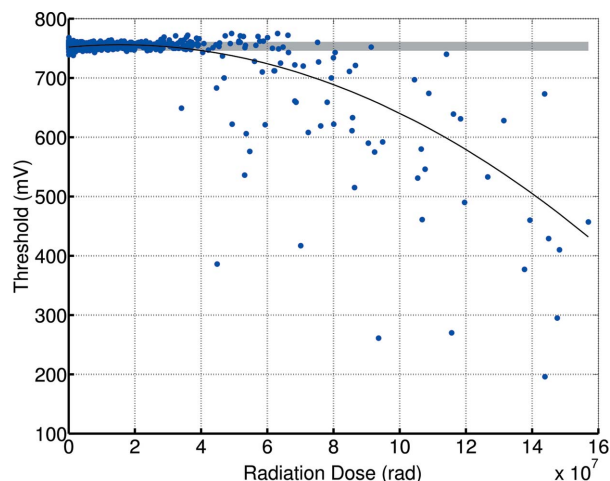


Figure 6 Absolute threshold values as a function of dose after re-trimming with the standard V_{trm} value 1.35 V. Minimal threshold dispersion and a retention of standard threshold values up to approximately 40 Mrad is evident.

this indicates that the magnitude of the threshold values is reduced by accumulated doses in excess of 30 Mrad. The observed shifts are considered permanent as rebound was not observed in the following fortnight. In order to aid in the interpretation of radiation-induced departure from nominal behaviour, a shaded 2σ variation band, representing the inherent threshold dispersion of un-irradiated pixels, has been included. The junction of the trend line with the variation band then yields an approximate indication of the dose required to cause departure from typical pixel behaviour.

4.1.3. Post-irradiation recalibration. Post-irradiation trimming was undertaken to determine whether the impact of radiation-induced threshold shifts could be minimized. A threshold scan was performed with the trimming circuitry enabled at the standard V_{trm} value of 1.35 V, the results of which are shown in Fig. 6. In comparison with Fig. 5, a slight reduction in threshold dispersion is observed. Furthermore, a

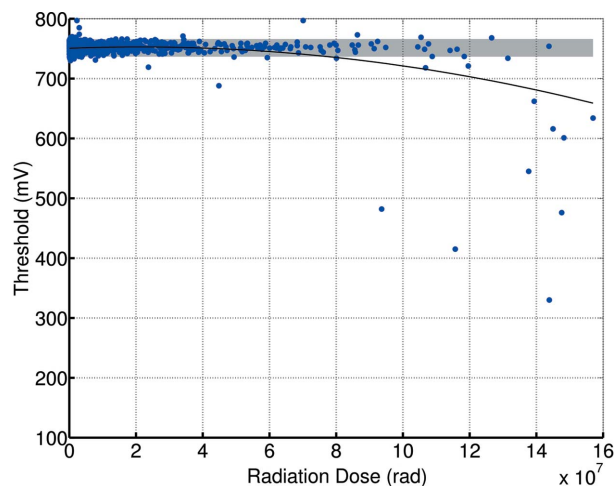


Figure 7 Absolute threshold values as a function of dose after re-trimming with a strong V_{trm} value of 1.25 V. Standard threshold values are retained up to approximately 80 Mrad; however, this is accompanied by a moderate increase in the threshold dispersion of un-irradiated pixels.

negligible threshold shift in irradiated pixels up to 40 Mrad is now present. To further investigate the use of trimming in the restoration of detector homogeneity post-irradiation, V_{trim} was decreased to 1.25 V. Reducing V_{trim} has the effect of increasing the range of the trimming procedure. The results obtained are presented in Fig. 7. Under these conditions, pixels that have received in excess of 80 Mrad can now be correctly compensated and retain standard thresholds. However, the cost of increasing the range of the trimming procedure is a slight increase in overall dispersion owing to quantization effects in the V_{trim} DAC.

5. Conclusions and outlook

It has been demonstrated that the PILATUS II sensor and read-out chip retain normal function up to a total sensor integrated dose of approximately 30 Mrad. Above this value, irradiation causes a clear increase in pixel sensitivity. By re-trimming the detector post-irradiation, pixels that receive a dose of up to 40 Mrad can also retain standard functionality. Furthermore, by strong re-trimming post-irradiation, radiation-induced threshold shifts caused by up to 80 Mrad can be countered. This procedure, however, leads to a slight increase in the threshold dispersion of un-irradiated pixels.

In a typical SAXS configuration, these findings confirm that the detector can be operated at 12 keV for in excess of 30 days at an individual pixel count rate of 10^6 counts s^{-1} . Re-trimming of the detector will enable retention of homogeneity for over 40 days of continuous exposure. In exceptional circumstances, further trimming has the potential to increase this to in excess of 80 days. Protein crystallographic measurements, where Bragg spots are randomly distributed, do not demand that individual pixels bear continuous high dose rates. This wider distribution of dose is therefore unlikely to compromise detector homogeneity, even under prolonged use.

Future chip fabrication utilizing a smaller CMOS process will greatly reduce the cross section of the SiO_2 interface, and therefore transistor susceptibility to radiation-induced threshold shifts.

This work was carried out with the financial support of a postgraduate overseas research experience scholarship provided by the Graduate Research Scholarships Office, The University of Melbourne.

References

- Anelli, G. (2000). PhD dissertation, Universite Montpellier II, Montpellier, France.
- Broennimann, Ch., Eikenberry, E. F., Henrich, B., Horisberger, R., Huelsen, G., Pohl, E., Schmitt, B., Schulze-Briese, C., Suzuki, M., Tomizaki, T., Toyokawa, H. & Wagner, A. (2006). *J. Synchrotron Rad.* **13**, 120–130.
- Broennimann, Ch., Florin, S., Lindner, M., Schmitt, B. & Schulze-Briese, C. (2000). *J. Synchrotron Rad.* **7**, 301–306.
- Broennimann, Ch., Glaus, F., Gobrecht, J., Heizing, S., Horisberger, M., Horisberger, R., Kastli, H. C., Lehmann, J., Rohe, T. & Streuli, S. (2006). *Nucl. Instrum. Methods Phys. Res. A*, **565**, 303–308.
- Dinapoli, R. (2004). PhD dissertation, Universite Montpellier II, Montpellier, France.
- Eikenberry, E. F., Broennimann, Ch., Hulsen, G., Toyokawa, H., Horisberger, R., Schmitt, B., Schulze-Briese, C., Tomizaki, T. & Wagner, A. (2003). *Nucl. Instrum. Methods Phys. Res. A*, **401**, 1–260.
- Lint, V. A. J. van, Flanagan, T. M., Leadon, R. E., Naber, J. A. & Rogers, V. C. (1980). *Mechanisms of Radiation Effects in Electronic Materials*, Vol. 1. Chichester: Wiley.
- Llopart, C. (2007). PhD dissertation, Mid Sweden University, Sundsvall, Sweden.
- McLean, F. B., Boesch, H. E. Jr & Oldham, T. R. (1989). *Electron-Hole Generation, Transport and Trapping in SiO_2* , in *Ionizing Radiation Effects in MOS Devices and Circuits*, ch. 1, edited by T. P. Ma and V. Dressendorfen. New York: John Wiley and Sons.
- Patterson, B. D. *et al.* (2005). *Nucl. Instrum. Methods Phys. Res. A*, **540**, 42–67.
- Rossi, L., Fischer, P., Rohe, T. & Wermes, N. (2006). *Pixel Detectors*. Berlin: Springer.
- Schlepütz, C. M., Herger, R., Willmott, P. R., Patterson, B. D., Bunk, O., Broennimann, Ch., Henrich, B., Hulsen, G. & Eikenberry, E. F. (2005). *Acta Cryst.* **A61**, 418–425.
- Winoukur, P. S. (1989). *Radiation-Induced Interface Traps*, in *Ionizing Radiation Effects in MOS Devices and Circuits*, ch. 4, edited by T. P. Ma and V. Dressendorfen. New York: John Wiley and Sons.